

Downscaled Representation Matters: Improving Image Rescaling with Collaborative Downscaled Images

Bingna Xu*, Yong Guo*, Luoqian Jiang, Mianjie Yu, Jian Chen[†]
South China University of Technology

sexbn@mail.scut.edu.cn, guoyongcs@gmail.com,
{seluoqianjiang, 202030482362}@mail.scut.edu.cn, ellachen@scut.edu.cn

Abstract

Deep networks have achieved great success in image rescaling (IR) task that seeks to learn the optimal downsampled representations, i.e., low-resolution (LR) images, to reconstruct the original high-resolution (HR) images. Compared with super-resolution methods that consider a fixed downscaling scheme, e.g., bicubic, IR often achieves significantly better reconstruction performance thanks to the learned downsampled representations. This highlights the importance of a good downsampled representation in image reconstruction tasks. Existing IR methods mainly learn the downsampled representation by jointly optimizing the downscaling and upscaling models. Unlike them, we seek to improve the downsampled representation through a different and more direct way – optimizing the downsampled image itself instead of the down-/upscaling models. Specifically, we propose a collaborative downscaling scheme that directly generates the collaborative LR examples by descending the gradient w.r.t. the reconstruction loss on them to benefit the IR process. Furthermore, since LR images are downsampled from the corresponding HR images, one can also improve the downsampled representation if we have a better representation in the HR domain. Inspired by this, we propose a **Hierarchical Collaborative Downscaling (HCD)** method that performs gradient descent in both HR and LR domains to improve the downsampled representations. Extensive experiments show that our HCD significantly improves the reconstruction performance both quantitatively and qualitatively. Moreover, we also highlight the flexibility of our HCD since it can generalize well across diverse IR models.

1. Introduction

Deep neural networks have achieved great success in many computer vision tasks, including image classifica-

* Authors contributed equally.

[†] Corresponding author.

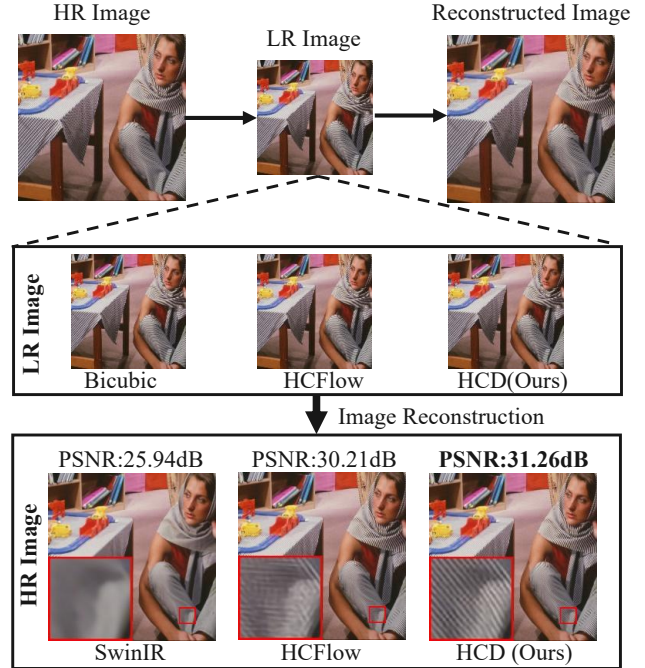


Figure 1. Image rescaling pipeline and the comparisons of the downsampled images along with the corresponding reconstructed HR images (4 \times). Top: we show the entire process of image rescaling. Middle: we visualize the downsampled representations used in different methods. Bottom: we compare the reconstructed HR images. With the improved downsampled representation, our method yields the best result both quantitatively and qualitatively.

tion [13, 16, 22, 24, 26, 55], semantic segmentation [40, 42, 58], and many other areas [7, 18, 23, 48, 49]. Recently, image rescaling has become an important task that seeks to downscale the high-resolution (HR) images to visually valid low-resolution (LR) images and then upscale them to recover the original HR images. In practice, the downsampled images play an important role in saving storage or bandwidth and fitting the screens with different resolutions [61], such as image/video compression and video communica-

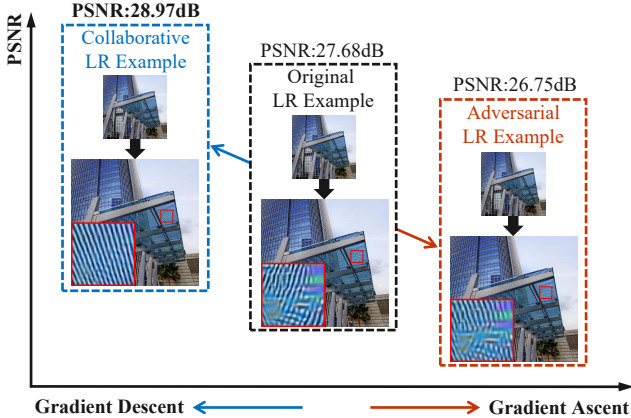


Figure 2. Comparison of adversarial examples and collaborative examples when producing downscaled representations. We ascend the gradient w.r.t the reconstruction loss to generate the adversarial examples. Based on the pretrained HCFlow model [36], the adversarial LR example yields lower PSNR along with distorted visual content in the reconstructed HR image. By contrast, we generate the collaborative LR example by descending the gradient and obtain significantly higher PSNR as well as better visual quality.

tion [51, 56, 66]. Interestingly, unlike super-resolution (SR) [3, 43, 54] methods that consider a fixed downscaling kernel, e.g., bicubic, IR often yields significantly better reconstruction performance [5, 25, 69] since IR essentially learns a better downscaled representation method. As shown in Figure 1, compared with a popular SR method SwinIR [35], the rescaling method HCFlow [36] greatly improves the PSNR score from 25.94 dB to 30.21 dB, which highlights the importance of a *good downscaled representation* in image reconstruction tasks.

To learn a good downscaled representation, existing IR methods jointly learn the downscaling and upscaling models by minimizing the reconstruction loss [36, 61]. Besides this line of research, one can also directly optimize the downscaled representation instead of updating the model parameters. From this point of view, a typical approach is adversarial attack that iteratively optimizes the input image itself to mislead the model [44]. Interestingly, adversarial attack is also very effective in image rescaling tasks. As shown in Figure 2, based on a popular IR model HCFlow [36], we apply gradient ascent on LR images to generate the adversarial example. In practice, it greatly hampers the reconstruction performance by reducing the PSNR by 0.93 dB and also introduces severe visual artifacts in the reconstructed HR image. The degraded performance encourages us to explore the possibility of improving reconstruction performance – optimizing the downscaled representation in an opposite way to adversarial attack.

Inspired by this, we propose a collaborative downscaling scheme that descends the gradient, i.e., reducing the

reconstruction loss, to construct the collaborative LR example. As shown in Figure 2, the collaborative example yields a significant performance improvement of 1.29 dB along with better visual details in the reconstructed image. Furthermore, since the LR image is obtained from the original HR image via downscaling, we can also improve the downsampled representation if we obtain a better representation in the HR domain, i.e., generating a collaborative HR example. Motivated by this, we propose a **Hierarchical Collaborative Downscaling (HCD)** scheme that optimizes the representations in both HR and LR domains to obtain a better downsampled example. Specifically, we first generate a collaborative example in the HR domain and use the downscaling model to obtain a downsampled image. Taking the downsampled image as an initialization point, we then generate the collaborative LR example to further improve the downsampled representation. Due to the dependence between HR and LR image (based on the downscaling process), the hierarchical collaborative learning scheme can be formulated by a bi-level optimization problem. In practice, we solve it by alternatively optimizing the representation in HR and LR domains. More critically, we highlight that the proposed HCD does not introduce extra computational overhead in the upscaling stage, making our method applicable to real-world scenarios. Extensive experiments show that our method greatly boosts the reconstruction performance with the help of the collaborative downscaled examples.

Our contributions are summarized as follows:

- We propose a novel collaborative image downscaling method that improves the image rescaling performance from a new perspective – learning a better downsampled representation. We highlight that, in the community of image reconstruction, it is the first attempt to directly optimize the downsampled representation instead of learning the downscaling or upscaling models to boost the performance of image rescaling.
- Since the low-resolution (LR) images strongly depend on the corresponding high-resolution (HR) images, we propose a Hierarchical Collaborative Downscaling (HCD) that optimizes the representations in both HR and LR domains to learn a better downsampled representation. We formulate the learning process as a bi-level optimization problem and solve it by alternatively generating collaborative HR and LR examples.
- Experiments on multiple benchmark datasets show that, on top of state-of-the-art image rescaling models, our HCD yields significantly better results both quantitatively and qualitatively. For example, based on a strong baseline HCFlow [36], we obtain a large PSNR improvement of 0.7 dB on Set5 for $4\times$ rescaling.

2. Related Work

2.1. Image Rescaling

Image rescaling (IR) and image super-resolution (SR) [6, 57, 64, 65] are distinct tasks. IR consists of image downscaling and image upscaling. SR corresponds to the latter process, which lacks a ground-truth HR image or any other prior information, and the reconstruction process is entirely based on the LR image. In contrast, we are given a ground-truth HR image in the IR task, but we must use its downscaled version for storage and transmission. We recover the original HR image when necessary. Image downscaling is the inverse of SR which generates the LR version of an HR image. The most common downscaling method is bicubic interpolation [46]. However, it will cause over-smoothed issues since the high-frequency details are suppressed. Furthermore, most image downscaling algorithms focus solely on the visual quality of the downsampled images, which may not be suitable for the upscaling tasks.

Recently, an increasing amount of work has been devoted to modeling image downscaling and upscaling as a unified task [12, 27, 33, 50, 59, 68]. Sun et al. [56] propose a content-adaptive resampler to achieve image downscaling and improves the upscaling model. Xiao et al. [61] propose a bidirectional image rescaling method based on invertible neural networks. Pan et al. [51] achieve bidirectional rescaling of arbitrary images by joint optimization. The above methods elaborately design the model architectures to reconstruct better images. Our method differs from them by directly optimizing the primeval input of the IR task under the supervision of the ground-truth HR image.

2.2. Image Super-Resolution

Image super-resolution (SR) is a widely-used image upscaling method that refers to recovering HR images from existing LR images. It is widely used in many applications, such as object detection [10], face recognition [47], medical imaging [29], and surveillance security [53]. Existing SR methods can be divided into three categories: interpolation-based, reconstruction-based, and learning-based methods. With the help of deep learning techniques, some SR methods achieve advanced effects on learning powerful prior information [9, 14, 19, 31, 34, 66, 67]. Ledig et al. [31] first propose SRGAN using Generative Adversarial Nets (GAN) [11] to solve the over-smoothed problem of the SR task. Zhang et al. [66] combine the channel attention mechanism with SR to improve the representation ability of the model. Li et al. [34] propose SRFBN to refine low-level information using high-level ones through feedback connections and learn better representations. Instead of manually designing SR models, many efforts [19] have been made to automatically devise effective SR architectures using the neural architecture search (NAS) tech-

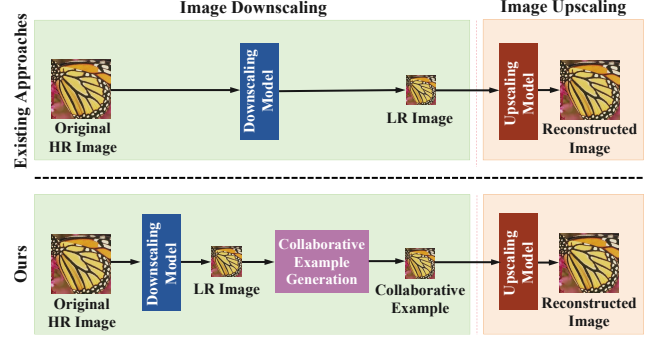


Figure 3. Comparison between existing image rescaling methods and the proposed HCD method. We additionally generate the collaborative LR examples to improve the downsampled representation while keeping the upscaling process unchanged.

niques [4, 15, 17]. Nevertheless, most existing SR models contain a large number of parameters and come with very high computational cost. To address this, some recent work exploit model compression techniques [39, 41, 70] to obtain compact SR models [21]. Compared with SR methods that consider a fixed downscaling scheme, existing IR methods often achieve significantly better reconstruction performance thanks to the learned downsampled representations.

2.3. Collaborative Example

Generating collaborative examples [32] and adversarial examples [20, 44] are a set of opposite processes. The adversarial attack refers to the process of generating an adversarial example by applying a minor perturbation to the original input and causing the model to make an incorrect inference. The gradient-based attack method increases the prediction loss by updating the example along the positive direction of the gradient. In contrast to the adversarial example, the collaborative example aims to improve the robustness of the model by updating the example along the negative direction of the gradient, which ultimately decreases the prediction loss of the model. Inspired by the collaborative example, we propose a hierarchical collaborative example generation algorithm to generate downsampled representation optimal for the upscaling model under the supervision of the HR image.

3. Collaborative Image Downscaling

In this paper, we seek to directly learn a better downsampled representation rather than the down-/upscaling models to improve the performance of reconstructed images. In Section 3.1, we first discuss the importance of downsampled representation in image reconstruction tasks. Besides learning a good model, directly optimizing the downsampled representation (purple box in Figure 3) is an effective way to improve performance. In Section 3.2, we further extend this idea and propose a Hierarchical Collaborative Downscaling

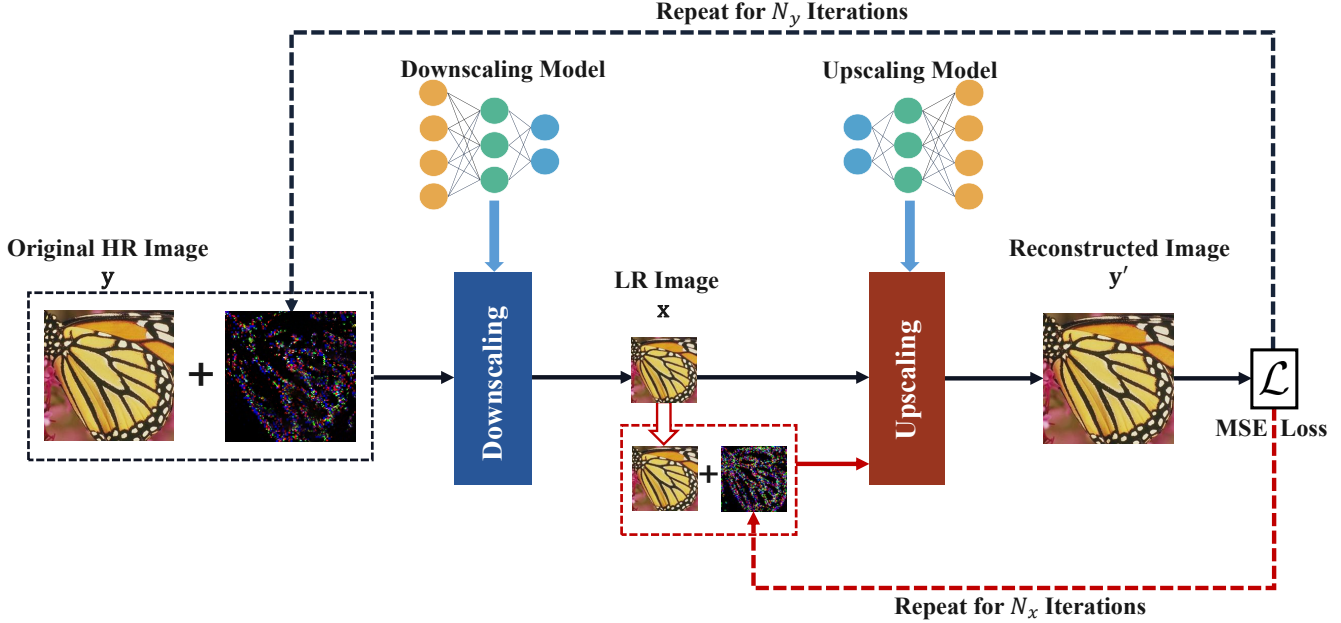


Figure 4. The proposed Hierarchical Collaborative Downscaling (HCD) scheme consists of two processes, including the collaborative HR example generation (marked as black lines) and the collaborative LR example generation (marked as red lines). We first iteratively optimize the perturbation on the original HR image to generate the collaborative HR examples. Then, we obtain the downsampled image and generate collaborative LR examples for it. In the end, we can get a better high-resolution image from the better downsampled representation.

(HCD) method that optimizes the representations in both high-resolution (HR) and low-resolution (LR) domains to obtain a better downsampled representation. The overview of our HCD method is shown in Figure 4.

3.1. Downsampled Representation Matters

Existing image rescaling (IR) methods [51, 56, 61] essentially learn the optimal downsampled representation by jointly training the downscaling and upscaling models to reconstruct the original HR images. Compared with super-resolution methods that consider a fixed downscaling kernel, e.g., bicubic, IR methods often yield significantly better results thanks to the improved downsampled representation. For example, as shown in Figure 1, a recent rescaling method HCFlow [36] outperforms a strong baseline by a large margin of 5.27 dB. Such a large performance gap indicates the importance of a good downsampled representation in image reconstruction tasks.

In order to improve the downsampled representation, all the existing rescaling methods learn a downscaling method to produce the LR images. Besides training the model, one can also directly optimize the downsampled representation itself. From this perspective, a popular approach is adversarial attack [52] that learns the optimal perturbations on data without changing the model parameters. As shown by the red box in Figure 2, the adversarial attacks against image rescaling models greatly hamper the reconstruction per-

formance in terms of both PSNR and visual quality. Nevertheless, we seek to improve the performance instead of degrading it. To address this issue, a simple and intuitive way is to generate collaborative examples by considering an opposite training objective to adversarial attack. Specifically, we seek to generate collaborative examples in the LR domain by minimizing the reconstruction loss. As shown by the blue box, we can simultaneously improve PSNR and obtain visually plausible details in the reconstructed HR image. We highlight that the PSNR improvement of 0.93 dB is significant in image reconstruction tasks and generating collaborative examples provides us with new insights.

3.2. Hierarchical Collaborative Downscaling

In this part, we further extend the above idea and propose a novel Hierarchical Collaborative Downscaling (HCD) scheme to improve the downsampled representation, as shown in Figure 4. It is worth noting that, since LR images are directly obtained from the corresponding HR images, one can also improve the LR representation based on a better example in the HR domain. In this way, it becomes possible to obtain a better downsampled representation by generating collaborative examples in both the LR and HR domains. Essentially, jointly learning both collaborative examples can be regarded as a bi-level optimization problem. Before discussing it, we first start with the generation of collaborative examples in each domain separately.

Generating collaborative LR examples. We first focus on the LR domain to generate collaborative examples. Basically, the standard image rescaling scheme seeks to map an HR image y to a downsampled image x and then upsample it to obtain a reconstructed HR image y' . To improve the reconstruction performance, we fix the model parameters and directly learn the optimal perturbation δ_x to improve the downsampled representation x . Let \mathcal{L} be the reconstruction loss, $f(\cdot)$, and $g(\cdot)$ denote the upscaling and downscaling model, respectively. Following [44], we constrain the perturbation within a p-norm epsilon ball to avoid significantly changing the visual content, i.e., $\|\delta_x\|_p \leq \epsilon$. Formally, the perturbations can be obtained by minimizing \mathcal{L} :

$$\delta_x = \arg \min_{\|\delta_x\|_p \leq \epsilon} \mathcal{L}(f(x + \delta_x), y). \quad (1)$$

Thus, the resultant downsampled representation can be obtained by summing up the original LR image and the learned perturbation via $x := x + \delta_x$.

Generating collaborative HR examples. Since the LR image x can be obtained by downscaling the HR image y , we can also generate a collaborative HR example to obtain a better downsampled representation. Similarly, we add additional perturbation δ_y to the input HR image y and optimize it by minimizing the reconstruction loss \mathcal{L} . Unlike Equation (1), we discard the perturbation in the LR domain and sequentially perform downscaling $g(\cdot)$ and upscaling $f(\cdot)$ to obtain the reconstructed image y' . Here, we consider the same constraint w.r.t. the epsilon ball. Thus, the perturbation in the HR domain can be obtained by

$$\delta_y = \arg \min_{\|\delta_y\|_p \leq \epsilon} \mathcal{L}(f(g(y + \delta_y)), y). \quad (2)$$

As illustrated above, we can obtain a better downsampled representation by generating either collaborative LR examples or collaborative HR examples. This motivates us to explore whether it is possible to further improve the downsampled representation if we combine them together. Inspired by this, we develop a hierarchical scheme that jointly optimizes the representations in both LR and HR domains. Due to the dependence of the LR image on the corresponding HR image, we consider a bi-level optimization problem to obtain the optimal LR perturbation:

$$\begin{aligned} \delta_x &= \arg \min_{\|\delta_x\|_p \leq \epsilon} \mathcal{L}(f(g(y + \delta_y) + \delta_x), y), \\ \text{s.t. } \delta_y &= \arg \min_{\|\delta_y\|_p \leq \epsilon} \mathcal{L}(f(g(y + \delta_y)), y). \end{aligned} \quad (3)$$

To solve this problem, we propose to alternatively generate collaborative examples in HR and LR domains. As shown in Algorithm 1, we first generate collaborative HR examples and downscale them to get the downsampled

Algorithm 1 Learning scheme of **Hierarchical Collaborative Downscaling (HCD)**. We present a hierarchical learning scheme that sequentially generates the collaborative HR examples and collaborative LR examples.

Input: HR image y , the downscaling model $g(\cdot)$, the upscaling model $f(\cdot)$, number of iterations N_y and N_x , perturbation budget ϵ , step size α , the clipping function to constrain the input within feasible range $Clip\{\cdot\}$.

Output: Reconstructed high-resolution image y' .

```

1: Initialize the perturbations  $\delta_y$  and  $\delta_x$ 
2: // Generate collaborative HR examples
3: for  $t = 1$  to  $N_y$  do
4:   Compute gradient via  $g = \nabla_{\delta_y} \mathcal{L}(f(g(y + \delta_y)), y)$ 
5:   Update  $\delta_y$  via  $\delta_y \leftarrow Clip\{\delta_y - \alpha * \frac{g}{\|g\|}, \epsilon\}$ 
6: end for
7: Obtain the collaborative HR example:  $y = y + \delta_y$ 
8: Compute low resolution images:  $x = g(y)$ 
9: // Generate collaborative LR examples
10: for  $t = 1$  to  $N_x$  do
11:   Obtain gradient via  $g = \nabla_{\delta_x} \mathcal{L}(f(x + \delta_x), y)$ 
12:   Update  $\delta_x$  via  $\delta_x \leftarrow Clip\{\delta_x - \alpha * \frac{g}{\|g\|}, \epsilon\}$ 
13: end for
14: Obtain the collaborative LR example:  $x = x + \delta_x$ 
15: Obtain the reconstructed image:  $y' = f(x)$ 

```

images. Then, we further generate collaborative examples w.r.t. the latest LR images to obtain the resultant downsampled representation. Following the optimization process of Project Gradient Descent (PGD) attack [44], we optimize the perturbations δ_x and δ_y in an iterative manner. For simplicity, we force both collaborative example generation processes to share the same number of iterations to perform gradient descent $N_x = N_y$. In this paper, we consider ℓ_2 -norm to build the epsilon ball, i.e., $p = 2$.

4. Experiments

In the experiments, we evaluate the effectiveness of HCD based on two popular image rescaling methods, including IRN [61] and HCFlow [36]. We first describe the implementation details in Section 4.1. Then, we compare our method with current advanced methods in Section 4.2 on informative quantitative and qualitative analyses. Finally, we conduct abundant ablation studies and raise further discussions in Section 4.3. Both our source code and all the collaborative examples along with the corresponding reconstruction images will be released soon.

4.1. Implementation Details

We evaluate the proposed HCD on the validation set of DIV2K [1] and four standard datasets, i.e., Set5 [2], Set14 [63], BSD100 [45], and Urban100 [28]. We com-

Method	Set5	Set14	BSD100	Urban100	DIV2K
Bicubic & Bicubic	28.42 / 0.8104	26.00 / 0.7027	25.96 / 0.6675	23.14 / 0.6577	26.66 / 0.8521
Bicubic & SRCNN [8]	30.48 / 0.8628	27.50 / 0.7513	26.90 / 0.7101	24.52 / 0.7221	–
Bicubic & RDN [67]	32.47 / 0.8990	28.81 / 0.7871	27.72 / 0.7419	26.61 / 0.8028	–
Bicubic & EDSR [37]	32.62 / 0.8984	28.94 / 0.7901	27.79 / 0.7437	26.86 / 0.8080	29.38 / 0.9032
Bicubic & RCAN [66]	32.63 / 0.9002	28.87 / 0.7889	27.77 / 0.7436	26.82 / 0.8087	30.77 / 0.8460
Bicubic & RFANet [38]	32.66 / 0.9004	28.88 / 0.7894	27.79 / 0.7442	26.92 / 0.8112	31.41 / 0.9187
Bicubic & RRDB [60]	32.74 / 0.9012	29.00 / 0.7915	27.84 / 0.7455	27.03 / 0.8152	30.92 / 0.8486
Bicubic & SwinIR [35]	32.72 / 0.9021	28.94 / 0.7914	27.83 / 0.7459	27.07 / 0.8164	–
TAD & TAU [30]	31.81 / –	28.63 / –	28.51 / –	26.63 / –	31.16 / –
CAR & EDSR [56]	33.88 / 0.9174	30.31 / 0.8382	29.15 / 0.8001	29.28 / 0.8711	32.82 / 0.8837
IRN [61]	36.19 / 0.9451	32.67 / 0.9015	31.64 / 0.8826	31.41 / 0.9157	35.07 / 0.9318
IRN+HCD ($N=15$)	36.63 / 0.9488	33.21 / 0.9076	32.03 / 0.8894	31.76 / 0.9180	35.20 / 0.9324
HCFlow [36]	36.29 / 0.9468	33.02 / 0.9065	31.74 / 0.8864	31.62 / 0.9206	35.32 / 0.9346
HCFlow+HCD ($N=15$)	36.99 / 0.9506	33.56 / 0.9116	32.22 / 0.8919	32.00 / 0.9231	35.36 / 0.9352

Table 1. Quantitative evaluation results (PSNR / SSIM) of image reconstruction on benchmark datasets with $4\times$ scale. The **black** values indicate the best result. HCD significantly improves. When the number of iterations $N=15$, our HCD-optimized IRN and HCFlow improve PSNR and SSIM metrics on each benchmark dataset.

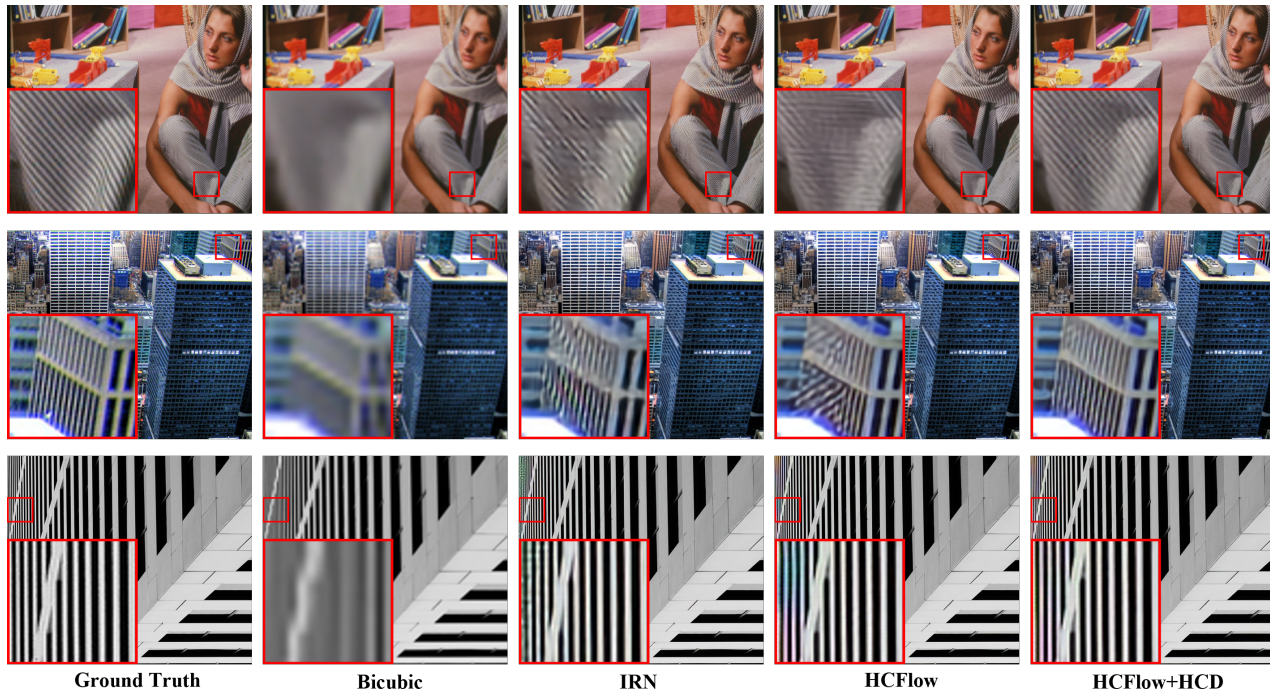


Figure 5. Qualitative results of upscaling the $4\times$ downsampled images. Our HCD with HCFlow is able to produce more realistic and sharper HR images compared with the baseline methods. See the appendix for more results.

pare HCD with several state-of-the-art methods, including IRN [61] and HCFlow [36]. Following [37], with regard to images in the YCbCr color space, we quantitatively evaluate the PSNR and SSIM [62] on the Y channel of them, and test in $2\times$ and $4\times$ scale downscaling and reconstruction. The perturbation budget ϵ is set to 0.3 and the inner step size α is set to 20/255 for all experiments. By default, the iteration numbers for constructing collaborative LR images N_x and HR images N_y are set to the same i.e. $N_x = N_y = 15$.

4.2. Comparisons with State-of-the-arts

This section reports the performance of image reconstruction results on PSNR and SSIM. We consider two kinds of reconstruction methods as our baselines: IR methods and SR methods, and experiment on the best-performing IR models with few iterations. It is worth mentioning that our HCD performs in the inference stage and the model parameters will not be changed during the iteration. We report

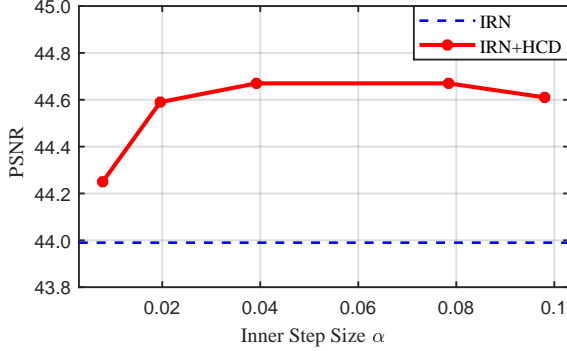


Figure 6. Experiment on choosing the different inner step sizes α on Set5 at $2\times$ scale at the 15th iteration based on IRN. Our HCD performs well by varying the inner step size from 0.04 to 0.08.

the quantitative evaluation result of $4\times$ scale and leave the results on $2\times$ scale in the appendix due to page limit. Our HCD significantly outperforms the baseline.

# Iterations N_x	# Iterations N_y	PSNR	SSIM
15	0	44.45	0.9880
0	15	44.37	0.9879
15	15	44.67	0.9886

Table 2. The quantitative evaluation results (PSNR / SSIM) of different iteration schemes on Set5 at $2\times$ scale based on IRN. Compared with optimizing LR or HR images separately (the second and third rows), the scheme of sequentially optimizing HR and LR images (the fourth row) increases PSNR by 0.22-0.30 dB.

Compared methods. To verify the effectiveness of our HCD, we investigate both IR methods and SR methods. IR methods includes HCFlow [36], IRN [61], TAD & TAU [30], CAR & EDSR [56]. As for SR methods, we use Bicubic downsampled LR images as input, and further perform SwinIR [35], RRDB [60], RFANet [38], RCAN [66], EDSR [37], RDN [67], SRCNN [8]. Compared with the above methods, our HCD has a great improvement in quantitative results and in qualitative results.

Quantitative results. We summarize the quantitative comparison results of HCD and other methods with $4\times$ scale in Table 1. Our HCD greatly achieves better performance than previous state-of-the-art methods on PSNR and SSIM in all datasets. When $N = 0$, it represents the initial results of the model. Compared with the original model, HCD significantly improves the reconstruction of HR images with 15 iterations. For the $4\times$ scale reconstructed images, HCD improves by 0.1-0.7 dB compared with HCFlow and improves by 0.2-0.44 dB on IRN. Especially, on dataset Set5, HCD achieves the PSNR metric of about 36.99 dB on

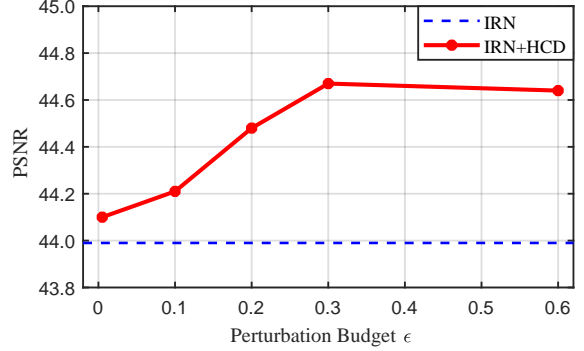


Figure 7. Experiment on choosing the different perturbation budget ϵ on Set5 at $2\times$ scale at the 15th iteration based on IRN. The perturbation budget ϵ is expected to be as small as possible to bring less perturbation while maintaining performance. A moderate value of $\epsilon = 0.3$ brings a significant improvement.

HCFlow. In general, our HCD significantly outperforms the baseline for PSNR and SSIM, respectively.

Qualitative results. We qualitatively evaluate our HCD by demonstrating details of the upscaled images. As shown in Figure 5, the results of HCD based on HCFlow achieve exhibit superior details and attractive visual quality. In the last set of Figure 5, our HCD alleviates unnatural colors in images from IRN and HCFlow. And it produces neater lines without bothersome horizontal lines compared with IRN. This demonstrates that our HCD significantly outperforms HCFlow and IRN visually.

4.3. Ablations and Further Discussions

In this section, we present the results of the various iteration schemes and iteration numbers, as well as the effects of inner step size α and perturbation budget ϵ . We also conduct ablations on HCD to justify each component. Unless otherwise specified, all ablation experiments are conducted on Set5 for $2\times$ scale based on IRN.

Effect of hierarchical collaborative learning. Table 2 reports the performance of different iteration combinations (N_x, N_y) based on the backbone method IRN. When the iteration number degrades to zero, we skip the collaborative example generation step for the HR or LR images, which corresponds to line 1 and line 3 in Table 2, respectively. When only collaborative LR examples or collaborative HR examples are used, the reconstructed image resolution is improved by 0.46 dB and 0.38 dB after 15 iterations compared to IRN. When we leverage both examples, we can improve the performance by 0.22-0.3 dB over the best results achieved by these two examples alone. These results demonstrate the effectiveness of the proposed hierarchical



Figure 8. Visualization of the generated collaborative LR examples (top) and the corresponding perturbations δ_x (bottom). The perturbations added to the LR image are mainly distributed on the contours and corners of the image. These visualization results indicate that the generated collaborative examples are able to provide more information for those high-frequency regions, which, however, are often hard to be reconstructed in the upscaling process.

# Iterations N	PSNR	SSIM	Downscaling Latency	Upscaling Latency
1	44.10	0.9872	0.33s	0.03s
5	44.52	0.9882	1.61s	
10	44.61	0.9884	2.98s	
15	44.67	0.9886	3.97s	
20	44.66	0.9872	5.26s	

Table 3. Effect of the number of iterations for generating collaborative examples ($N_x = N_y = N$) on the reconstruction performance and computational cost. We report results on Set5 for $2\times$ rescaling based on IRN. Our HCD method gradually improves the reconstruction performance when we increase the number of collaborative iterations from 1 to 15. Nevertheless, the performance improvement becomes negligible if we further increase the iteration number to $N = 20$. More critically, we highlight that our method does not increase the latency of the upscaling stage, which makes it applicable in real-world scenarios.

learning scheme, showing that the collaborative HR examples can be combined with the collaborative LR examples to boost the image reconstruction performance.

Effect of the step size α . In order to explore the effect of different inner step size α , we keep the perturbation budget ϵ fixed at 0.3 and change the α in a range on IRN. The inference results are shown in Figure 6. Similar to the learning rate, if it is too low, the inference process will converge slowly, causing the LR and HR images we infer to be lower than expected. However, since we randomly initialize the perturbations, a too-high α can also produce unreliable results. Experimental results show that our HCD performs well by varying the inner step size from 0.04 to 0.08.

Effect of the perturbation budget ϵ . As shown in Figure 7, We show how the inference results change as the perturbation budget changes. The maximum change in the

image over the course of one iteration is related to the perturbation budget. As the figure illustrates, due to the limit of the change, a low perturbation budget can not produce a very good performance. The high perturbation budget allows for a wide range of pixel variations, resulting dramatically image changes, so it causes subpar performance. We aim to achieve excellent performance improvement with minimal changes to the original images.

Visualization of generated perturbations on LR images.

In this section, we explicitly visualize the generated perturbations on the downsampled representation, i.e., δ_x in Eq. (3). As shown in Figure 8, the perturbations are mainly distributed on the contour and corner of the image, such as the woman’s eyes and the structure of a butterfly. Interestingly, these regions often contain high-frequency information that is hard to capture in the image upscaling process. We highlight that the performance improvement of our HCD method mainly stems from these collaborative perturbations.

Effect of the collaborative iteration number N . In Table 3, we choose IRN as our backbone method and study the effect of different values of collaborative iteration number N on building our collaborative example. In the default setting, we suggest $N_x = N_y = N$. We can find that the performance of IRN+HCD improves as the number of iterations increases, and only a few iterations are required to achieve a stable and satisfactory reconstruction effect. Additionally, we report the downscaling and upscaling latency and find that running 15 iterations only takes 3.97 s during the downscaling stage. Since our method does not increase the latency of the upscaling stage, which makes it is applicable in real-world scenarios.

5. Conclusion

In this paper, we propose a Hierarchical Collaborative Downscaling (HCD) method for the image rescaling task. In the first step, we generate collaborative samples for the input HR image of the downscaling model, so that it can be downsampled into a better LR representation. Then, we generate collaborative samples for the optimized LR to further improve its reconstruction performance. Extensive experiments show, both quantitatively and qualitatively, that our HCD significantly improves the performance on top of diverse image rescaling models.

References

- [1] Eirikur Agustsson and Radu Timofte. Ntire 2017 challenge on single image super-resolution: Dataset and study. In *Proceedings of the IEEE conference on computer vision and pattern recognition workshops*, pages 126–135, 2017. 5
- [2] Marco Bevilacqua, Aline Roumy, Christine Guillemot, and Marie-Line Alberi-Morel. Low-complexity single-image super-resolution based on nonnegative neighbor embedding. In *BMVC*, 2012. 5
- [3] Honggang Chen, Xiaohai He, Linbo Qing, Yuanyuan Wu, Chao Ren, Ray E Sheriff, and Ce Zhu. Real-world single image super-resolution: A brief review. *Information Fusion*, 79:124–145, 2022. 2
- [4] Yaofo Chen, Yong Guo, Qi Chen, Minli Li, Wei Zeng, Yaowei Wang, and Mingkui Tan. Contrastive neural architecture search with neural architecture comparators. In *Proceedings of the IEEE/CVF Conference on Computer Vision and Pattern Recognition*, pages 9502–9511, 2021. 3
- [5] Yan-An Chen, Ching-Chun Hsiao, Wen-Hsiao Peng, and Ching-Chun Huang. Direct: Discrete image rescaling with enhancement from case-specific textures. In *2021 International Conference on Visual Communications and Image Processing (VCIP)*, pages 1–5. IEEE, 2021. 2
- [6] Tao Dai, Jianrui Cai, Yongbing Zhang, Shu-Tao Xia, and Lei Zhang. Second-order attention network for single image super-resolution. In *Proceedings of the IEEE/CVF conference on computer vision and pattern recognition*, pages 11065–11074, 2019. 3
- [7] Qinyi Deng, Yong Guo, Zhibang Yang, Haolin Pan, and Jian Chen. Boosting semi-supervised learning with contrastive complementary labeling. *arXiv preprint*, 2022. 1
- [8] Chao Dong, Chen Change Loy, Kaiming He, and Xiaoou Tang. Learning a deep convolutional network for image super-resolution. In *ECCV*, 2014. 6, 7
- [9] Chao Dong, Chen Change Loy, Kaiming He, and Xiaoou Tang. Image super-resolution using deep convolutional networks. *IEEE transactions on pattern analysis and machine intelligence*, 38(2):295–307, 2015. 3
- [10] Ross Girshick, Jeff Donahue, Trevor Darrell, and Jitendra Malik. Region-based convolutional networks for accurate object detection and segmentation. *IEEE transactions on pattern analysis and machine intelligence*, 38(1):142–158, 2015. 3
- [11] Ian Goodfellow, Jean Pouget-Abadie, Mehdi Mirza, Bing Xu, David Warde-Farley, Sherjil Ozair, Aaron Courville, and Yoshua Bengio. Generative adversarial networks. *Communications of the ACM*, 63(11):139–144, 2020. 3
- [12] Mengxi Guo, Shijie Zhao, Yue Li, Junlin Li, Li Zhang, and Yue Wang. Invertible single image rescaling via steganography. In *2022 IEEE International Conference on Multimedia and Expo (ICME)*, pages 1–6. IEEE, 2022. 3
- [13] Yong Guo, Jian Chen, Qing Du, Anton Van Den Hengel, Qinfeng Shi, and Mingkui Tan. Multi-way backpropagation for training compact deep neural networks. *Neural networks*, 126:250–261, 2020. 1
- [14] Yong Guo, Jian Chen, Jingdong Wang, Qi Chen, Jiezhong Cao, Zeshuai Deng, Yanwu Xu, and Mingkui Tan. Closed-loop matters: Dual regression networks for single image super-resolution. In *Proceedings of the IEEE/CVF conference on computer vision and pattern recognition*, pages 5407–5416, 2020. 3
- [15] Yong Guo, Qi Chen, Jian Chen, Qingyao Wu, Qinfeng Shi, and Mingkui Tan. Auto-embedding generative adversarial networks for high resolution image synthesis. *IEEE Transactions on Multimedia*, 21(11):2726–2737, 2019. 3
- [16] Yong Guo, Yaofo Chen, Mingkui Tan, Kui Jia, Jian Chen, and Jingdong Wang. Content-aware convolutional neural networks. *Neural Networks*, 143:657–668, 2021. 1
- [17] Yong Guo, Yaofo Chen, Yin Zheng, Qi Chen, Peilin Zhao, Jian Chen, Junzhou Huang, and Mingkui Tan. Pareto-aware neural architecture generation for diverse computational budgets. *arXiv preprint arXiv:2210.07634*, 2022. 3
- [18] Yong Guo, Yaofo Chen, Yin Zheng, Peilin Zhao, Jian Chen, Junzhou Huang, and Mingkui Tan. Breaking the curse of space explosion: Towards efficient nas with curriculum search. In *International Conference on Machine Learning*, pages 3822–3831. PMLR, 2020. 1
- [19] Yong Guo, Yongsheng Luo, Zhenhao He, Jin Huang, and Jian Chen. Hierarchical neural architecture search for single image super-resolution. *IEEE Signal Processing Letters*, 27:1255–1259, 2020. 3
- [20] Yong Guo, David Stutz, and Bernt Schiele. Improving robustness by enhancing weak subnets. In *European Conference on Computer Vision*, pages 320–338. Springer, 2022. 3

- [21] Yong Guo, Jingdong Wang, Qi Chen, Jiezhong Cao, Zeshuai Deng, Yanwu Xu, Jian Chen, and Minghui Tan. Towards lightweight super-resolution with dual regression learning. *arXiv preprint arXiv:2207.07929*, 2022. 3
- [22] Yong Guo, Qingyao Wu, Chaorui Deng, Jian Chen, and Minghui Tan. Double forward propagation for memorized batch normalization. In *Proceedings of the AAAI Conference on Artificial Intelligence*, volume 32, 2018. 1
- [23] Yong Guo, Yin Zheng, Minghui Tan, Qi Chen, Jian Chen, Peilin Zhao, and Junzhou Huang. Nat: Neural architecture transformer for accurate and compact architectures. *Advances in Neural Information Processing Systems*, 32, 2019. 1
- [24] Yong Guo, Yin Zheng, Minghui Tan, Qi Chen, Zhipeng Li, Jian Chen, Peilin Zhao, and Junzhou Huang. Towards accurate and compact architectures via neural architecture transformer. *IEEE Transactions on Pattern Analysis and Machine Intelligence*, 2021. 1
- [25] Kamali Gupta, Atul Garg, Vinay Kukreja, and Deepali Gupta. Rice diseases multi-classification: An image resizing deep learning approach. In *2021 International Conference on Decision Aid Sciences and Application (DASA)*, pages 170–175. IEEE, 2021. 2
- [26] Kaiming He, Xiangyu Zhang, Shaoqing Ren, and Jian Sun. Deep residual learning for image recognition. In *Proceedings of the IEEE conference on computer vision and pattern recognition*, pages 770–778, 2016. 1
- [27] Xianxu Hou, Yuanhao Gong, Bozhi Liu, Ke Sun, Jingxin Liu, Bolei Xu, Jiang Duan, and Guoping Qiu. Learning based image transformation using convolutional neural networks. *IEEE Access*, 6:49779–49792, 2018. 3
- [28] Jia-Bin Huang, Abhishek Singh, and Narendra Ahuja. Single image super-resolution from transformed self-exemplars. *2015 IEEE Conference on Computer Vision and Pattern Recognition (CVPR)*, pages 5197–5206, 2015. 5
- [29] Yawen Huang, Ling Shao, and Alejandro F Frangi. Simultaneous super-resolution and cross-modality synthesis of 3d medical images using weakly-supervised joint convolutional sparse coding. In *Proceedings of the IEEE conference on computer vision and pattern recognition*, pages 6070–6079, 2017. 3
- [30] Heewon Kim, Myungsub Choi, Bee Lim, and Kyoung Mu Lee. Task-aware image downscaling. In *Proceedings of the European Conference on Computer Vision (ECCV)*, pages 399–414, 2018. 6, 7
- [31] Christian Ledig, Lucas Theis, Ferenc Huszár, Jose Caballero, Andrew Cunningham, Alejandro Acosta, Andrew Aitken, Alykhan Tejani, Johannes Totz, Zehan Wang, et al. Photo-realistic single image super-resolution using a generative adversarial network. In *Proceedings of the IEEE conference on computer vision and pattern recognition*, pages 4681–4690, 2017. 3
- [32] Qizhang Li, Yiwen Guo, Wangmeng Zuo, and Hao Chen. Collaborative adversarial training. *arXiv preprint arXiv:2205.11156*, 2022. 3
- [33] Shang Li, Guixuan Zhang, Zhengxiong Luo, Jie Liu, Zhi Zeng, and Shuwu Zhang. Approaching the limit of image rescaling via flow guidance. *arXiv preprint arXiv:2111.05133*, 2021. 3
- [34] Zhen Li, Jinglei Yang, Zheng Liu, Xiaomin Yang, Gwanggil Jeon, and Wei Wu. Feedback network for image super-resolution. In *Proceedings of the IEEE/CVF conference on computer vision and pattern recognition*, pages 3867–3876, 2019. 3
- [35] Jingyun Liang, Jiezhong Cao, Guolei Sun, Kai Zhang, Luc Van Gool, and Radu Timofte. Swinir: Image restoration using swin transformer. In *Proceedings of the IEEE/CVF International Conference on Computer Vision*, pages 1833–1844, 2021. 2, 6, 7
- [36] Jingyun Liang, Andreas Lugmayr, K. Zhang, Martin Danelljan, Luc Van Gool, and Radu Timofte. Hierarchical conditional flow: A unified framework for image super-resolution and image rescaling. *2021 IEEE/CVF International Conference on Computer Vision (ICCV)*, pages 4056–4065, 2021. 2, 4, 5, 6, 7
- [37] Bee Lim, Sanghyun Son, Heewon Kim, Seungjun Nah, and Kyoung Mu Lee. Enhanced deep residual networks for single image super-resolution. *2017 IEEE Conference on Computer Vision and Pattern Recognition Workshops (CVPRW)*, pages 1132–1140, 2017. 6, 7
- [38] Jie Liu, Wenjie Zhang, Yu Tang, Jie Tang, and Gangshan Wu. Residual feature aggregation network for image super-resolution. *2020 IEEE/CVF Conference on Computer Vision and Pattern Recognition (CVPR)*, pages 2356–2365, 2020. 6, 7
- [39] Jing Liu, Bohan Zhuang, Zhuangwei Zhuang, Yong Guo, Junzhou Huang, Jinhui Zhu, and Minghui Tan. Discrimination-aware network pruning for deep model compression. *IEEE Transactions on Pattern Analysis and Machine Intelligence*, 2021. 3
- [40] Lihao Liu, Junyi Cao, Minqian Liu, Yong Guo, Qi Chen, and Minghui Tan. Dynamic extension nets for few-shot semantic segmentation. In *Proceedings of the 28th ACM international conference on multimedia*, pages 1441–1449, 2020. 1
- [41] Yixin Liu, Yong Guo, Jiaxin Guo, Luoqian Jiang, and Jian Chen. Conditional automated channel pruning for deep neural networks. *IEEE Signal Processing Letters*, 28:1275–1279, 2021. 3
- [42] Jonathan Long, Evan Shelhamer, and Trevor Darrell. Fully convolutional networks for semantic segmentation. In *Proceedings of the IEEE conference on computer vision and pattern recognition*, pages 3431–3440, 2015. 1
- [43] Zhisheng Lu, Juncheng Li, Hong Liu, Chaoyan Huang, Linlin Zhang, and Tieyong Zeng. Transformer for single image super-resolution. In *Proceedings of the IEEE/CVF Conference on Computer Vision and Pattern Recognition*, pages 457–466, 2022. 2
- [44] Aleksander Madry, Aleksandar Makelov, Ludwig Schmidt, Dimitris Tsipras, and Adrian Vladu. Towards deep learning models resistant to adversarial attacks. *arXiv preprint arXiv:1706.06083*, 2017. 2, 3, 5
- [45] David R. Martin, Charles C. Fowlkes, Doron Tal, and Jitendra Malik. A database of human segmented natural images

- and its application to evaluating segmentation algorithms and measuring ecological statistics. *Proceedings Eighth IEEE International Conference on Computer Vision. ICCV 2001*, 2:416–423 vol.2, 2001. 5
- [46] Don P Mitchell and Arun N Netravali. Reconstruction filters in computer-graphics. *ACM Siggraph Computer Graphics*, 22(4):221–228, 1988. 3
- [47] Sivaram Prasad Mudunuri and Soma Biswas. Low resolution face recognition across variations in pose and illumination. *IEEE transactions on pattern analysis and machine intelligence*, 38(5):1034–1040, 2015. 3
- [48] Shuaicheng Niu, Jiaxiang Wu, Guanghui Xu, Yifan Zhang, Yong Guo, Peilin Zhao, Peng Wang, and Mingkui Tan. Adaxpert: Adapting neural architecture for growing data. In *International Conference on Machine Learning*, pages 8184–8194. PMLR, 2021. 1
- [49] Haolin Pan, Yong Guo, Qinyi Deng, Haomin Yang, Yiqun Chen, and Jian Chen. Improving fine-tuning of self-supervised models with contrastive initialization. *arXiv preprint arXiv:2208.00238*, 2022. 1
- [50] Zhihong Pan. Learning adjustable image rescaling with joint optimization of perception and distortion. In *ICASSP 2022-2022 IEEE International Conference on Acoustics, Speech and Signal Processing (ICASSP)*, pages 2455–2459. IEEE, 2022. 3
- [51] Zhihong Pan, Baopu Li, Dongliang He, Mingde Yao, Wenhao Wu, Tianwei Lin, Xin Li, and Errui Ding. Towards bidirectional arbitrary image rescaling: Joint optimization and cycle idempotence. In *Proceedings of the IEEE/CVF Conference on Computer Vision and Pattern Recognition*, pages 17389–17398, 2022. 2, 3, 4
- [52] Shilin Qiu, Qihe Liu, Shijie Zhou, and Chunjiang Wu. Review of artificial intelligence adversarial attack and defense technologies. *Applied Sciences*, 9(5):909, 2019. 4
- [53] Pejman Rasti, Tonis Uiboupin, Sergio Escalera, and Gholamreza Anbarjafari. Convolutional neural network super resolution for face recognition in surveillance monitoring. In *International conference on articulated motion and deformable objects*, pages 175–184. Springer, 2016. 3
- [54] Chitwan Saharia, Jonathan Ho, William Chan, Tim Salimans, David J Fleet, and Mohammad Norouzi. Image super-resolution via iterative refinement. *IEEE Transactions on Pattern Analysis and Machine Intelligence*, 2022. 2
- [55] Karen Simonyan and Andrew Zisserman. Very deep convolutional networks for large-scale image recognition. *arXiv preprint arXiv:1409.1556*, 2014. 1
- [56] Wanjie Sun and Zhenzhong Chen. Learned image downscaling for upscaling using content adaptive resampler. *IEEE Transactions on Image Processing*, 29:4027–4040, 2020. 2, 3, 4, 6, 7
- [57] Tong Tong, Gen Li, Xiejie Liu, and Qinquan Gao. Image super-resolution using dense skip connections. In *Proceedings of the IEEE international conference on computer vision*, pages 4799–4807, 2017. 3
- [58] Panqu Wang, Pengfei Chen, Ye Yuan, Ding Liu, Zehua Huang, Xiaodi Hou, and Garrison Cottrell. Understanding convolution for semantic segmentation. In *2018 IEEE winter conference on applications of computer vision (WACV)*, pages 1451–1460. Ieee, 2018. 1
- [59] Qing Wang, Heidi R Howard, Juliana M Mcmillan, Guangxing Wang, and Xiaoyu Xu. A cnn-based rescaling algorithm and performance analysis for spatial resolution enhancement of landsat images. *International Journal of Remote Sensing*, 43(2):607–629, 2022. 3
- [60] Xintao Wang, Ke Yu, Shixiang Wu, Jinjin Gu, Yihao Liu, Chao Dong, Chen Change Loy, Yu Qiao, and Xiaoou Tang. Esrgan: Enhanced super-resolution generative adversarial networks. In *ECCV Workshops*, 2018. 6, 7
- [61] Mingqing Xiao, Shuxin Zheng, Chang Liu, Yaolong Wang, Di He, Guolin Ke, Jiang Bian, Zhouchen Lin, and Tie-Yan Liu. Invertible image rescaling. In *European Conference on Computer Vision*, pages 126–144. Springer, 2020. 1, 2, 3, 4, 5, 6, 7
- [62] Hyunho Yeo, Youngmok Jung, Jaehong Kim, Jinwoo Shin, and Dongsu Han. Neural adaptive content-aware internet video delivery. In *OSDI*, 2018. 6
- [63] Roman Zeyde, Michael Elad, and Matan Protter. On single image scale-up using sparse-representations. In *Curves and Surfaces*, 2010. 5
- [64] Kai Zhang, Wangmeng Zuo, and Lei Zhang. Learning a single convolutional super-resolution network for multiple degradations. In *Proceedings of the IEEE conference on computer vision and pattern recognition*, pages 3262–3271, 2018. 3
- [65] Kai Zhang, Wangmeng Zuo, and Lei Zhang. Deep plug-and-play super-resolution for arbitrary blur kernels. In *Proceedings of the IEEE/CVF Conference on Computer Vision and Pattern Recognition*, pages 1671–1681, 2019. 3
- [66] Yulun Zhang, Kunpeng Li, Kai Li, Lichen Wang, Bineng Zhong, and Yun Fu. Image super-resolution using very deep residual channel attention networks. In *Proceedings of the European conference on computer vision (ECCV)*, pages 286–301, 2018. 2, 3, 6, 7
- [67] Yulun Zhang, Yapeng Tian, Yu Kong, Bineng Zhong, and Yun Fu. Residual dense network for image super-resolution. In *Proceedings of the IEEE conference on computer vision and pattern recognition*, pages 2472–2481, 2018. 3, 6, 7
- [68] Zhixuan Zhong, Liangyu Chai, Yang Zhou, Bailin Deng, Jia Pan, and Shengfeng He. Faithful extreme rescaling via generative prior reciprocated invertible representations. In *Proceedings of the IEEE/CVF Conference on Computer Vision and Pattern Recognition*, pages 5708–5717, 2022. 3
- [69] Yiming Zhu, Cairong Wang, Chenyu Dong, Ke Zhang, Hongyang Gao, and Chun Yuan. High-frequency normalizing flow for image rescaling. *IEEE Transactions on Image Processing*, 2022. 2
- [70] Zhuangwei Zhuang, Mingkui Tan, Bohan Zhuang, Jing Liu, Yong Guo, Qingyao Wu, Junzhou Huang, and Jinhui Zhu. Discrimination-aware channel pruning for deep neural networks. *Advances in neural information processing systems*, 31, 2018. 3